Electronic Supplementary Information

for

Relationships among structural topology, bond strength, and mechanical properties of single-walled aluminosilicate nanotubes

Kai-Hsin Liou,[a] *Nien-Ti Tsou*[b] *and Dun-Yen Kang**[a]

[a]Department of Chemical Engineering, National Taiwan University

No. 1, Sec. 4, Roosevelt Road, Taipei 10617, Taiwan

[b]Department of Materials Science and Engineering, National Chiao Tung University

No. 1001, University Road, Hsinchu 30010, Taiwan

* E-mail: dunyen@ntu.edu.tw

A) Effects of Convergence Levels on Geometry Optimization of the Structure and Mechanical Properties of AlSiNT

We evaluated the correlation between the level of convergence in geometry optimization and the resulting elastic modulus of nanotubes (AlSiNT11, length = 21.25 nm). Table S1 details the settings of various convergence levels.

Table S1. Settings of various convergence levels

	Energy tolerance (eV/atom)	Maximum force (eV/Å)	Maximum displacement (Å)
Fine*	0.00001	0.03	0.001
Coarse	0.00005	0.1	0.005
Medium	0.00002	0.05	0.002
Fine	0.00001	0.03	0.001
Ultrafine	0.000005	0.01	0.0005

* Optimization of geometry was performed using the "fine" level but conducted only on a unit cell of gibbsite (the building block of the nanotubes), rather than a complete nanotube model. All other convergence levels listed in this table are applicable to the optimization of geometry in a complete nanotube model.

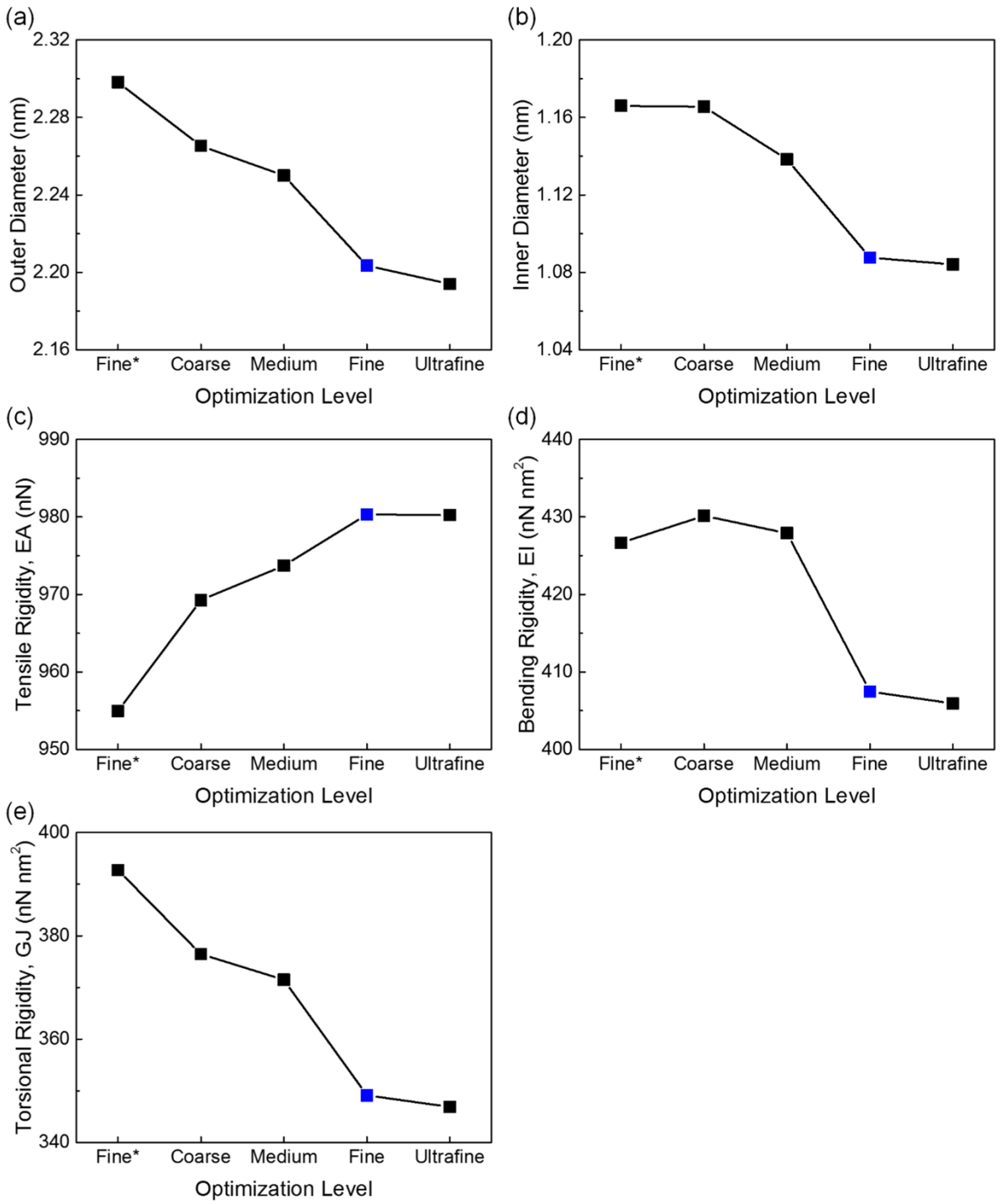

Fig. S1 (a) Outer diameter, (b) inner diameter, (c) tensile rigidity, (d) bending rigidity, and (e) torsional rigidity of AlSiNT11 under various convergence levels. The results begin to converge at the "fine" convergence level (marked in blue); therefore, we adopted this for all simulations presented in the manuscript.

B) Poisson's Ratio Effects

Poisson's ratio was assumed to be 0 for all simulations presented in the manuscript. In Fig. S2, it can be seen that three elastic moduli remain nearly unchanged in the range from 0 to 0.5, which is a typical range for most existing materials.

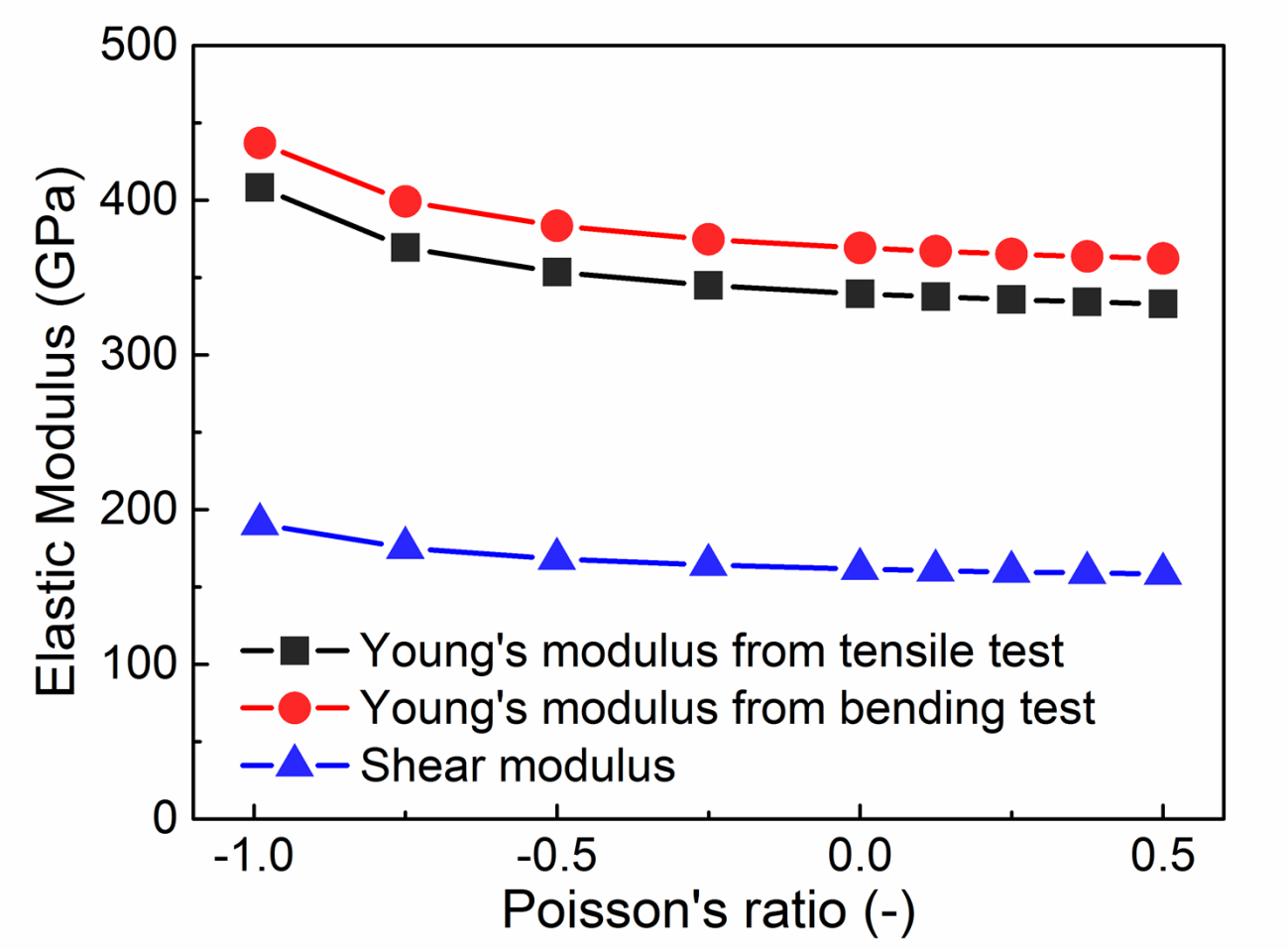

Fig. S2 Elastic moduli of AlSiNT12 (length = 17 nm) from various simulated tests with various Poisson ratios

Table S2. Force constant, Young's modulus, and diameter of each type of beam element

	k_r (nN/nm)	k_θ (nN nm/rad^2)	E_b (GPa)	d_b (Å)
Al-O	273	0.697	1631	2.02
Si-O	273	0.697	1397	2.02
O-H	376	0.231	4738	0.993
carbon-carbon[1]	652	0.876	5488	1.47

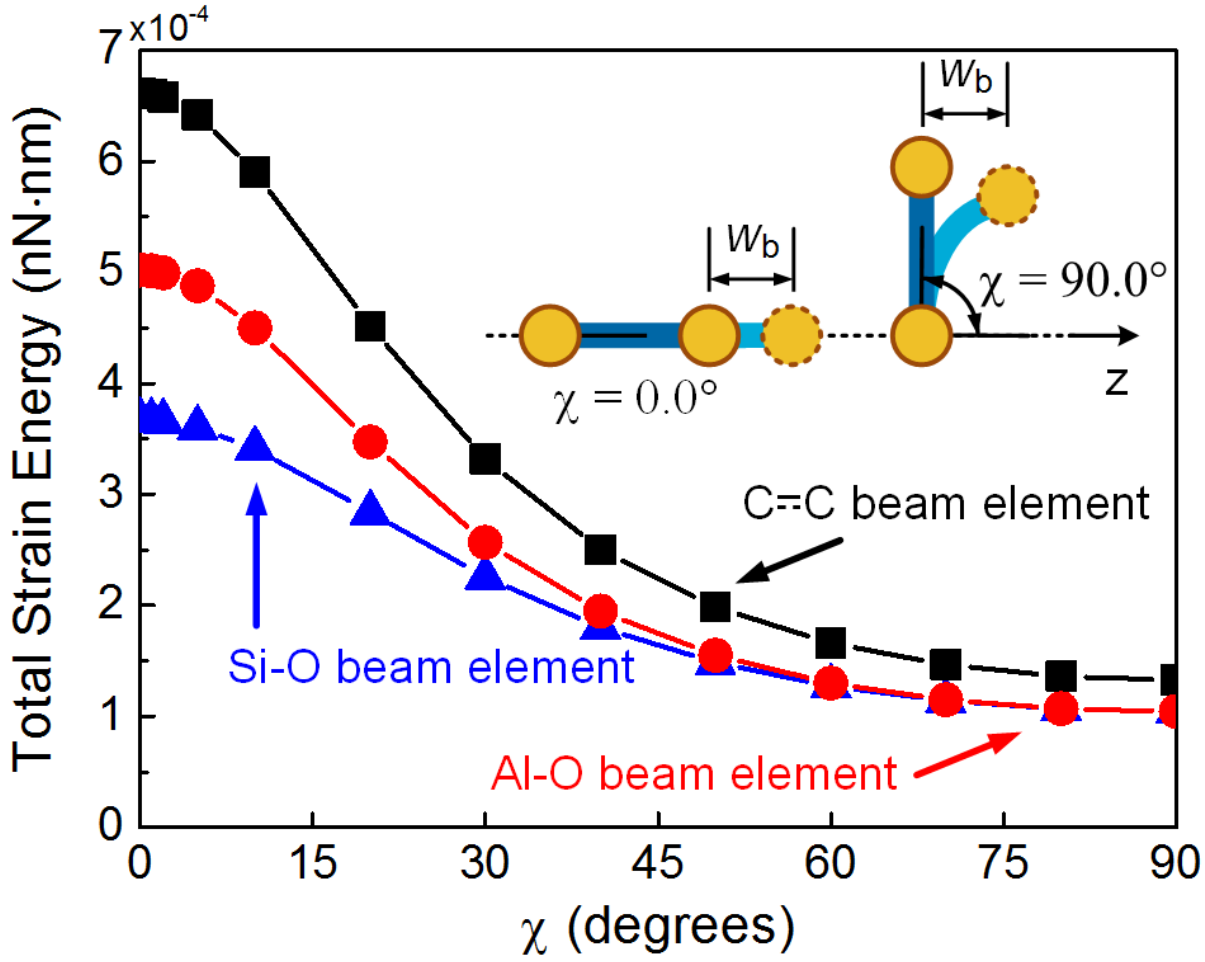

Fig. S3 Total strain energy of carbon-carbon, Al-O, and Si-O beam elements as a function of χ with one end of the beam fixed and the other end subject to displacement (w_b) along the z-axis

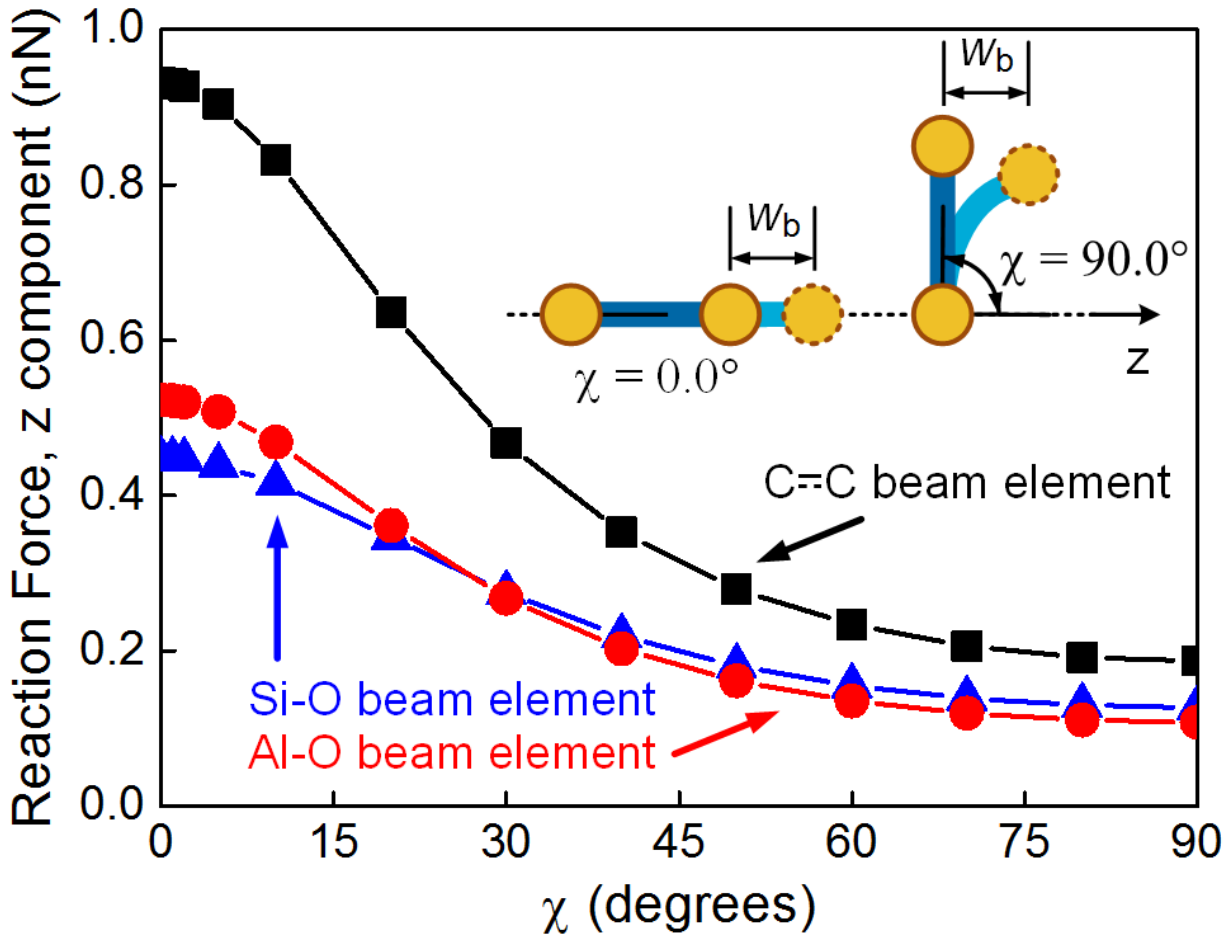

Fig. S4 z component of reaction force of carbon-carbon, Al-O, and Si-O beam elements as a function of χ with one end of the beam fixed and the other end subject to displacement (w_b) along the z-axis

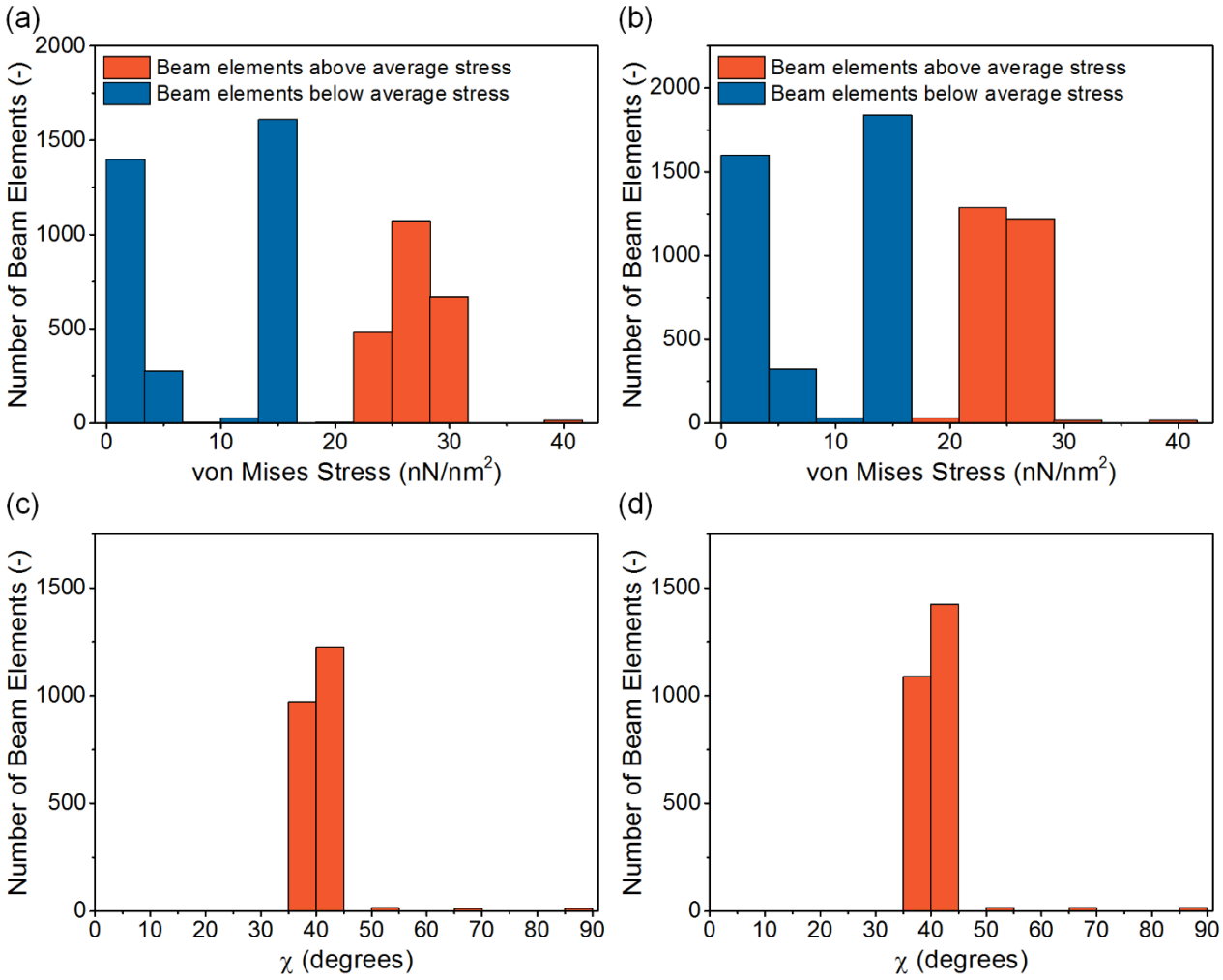

Fig. S5 von Mises stress distribution in (a) AlSiNT14 (length = 8.5 nm) and (b) AlSiNT16 (length = 8.5 nm). χ distributions of beam elements with above average von Mises stress for (c) AlSiNT14 (length = 8.5 nm) and (d) AlSiNT16 (length = 8.5 nm).

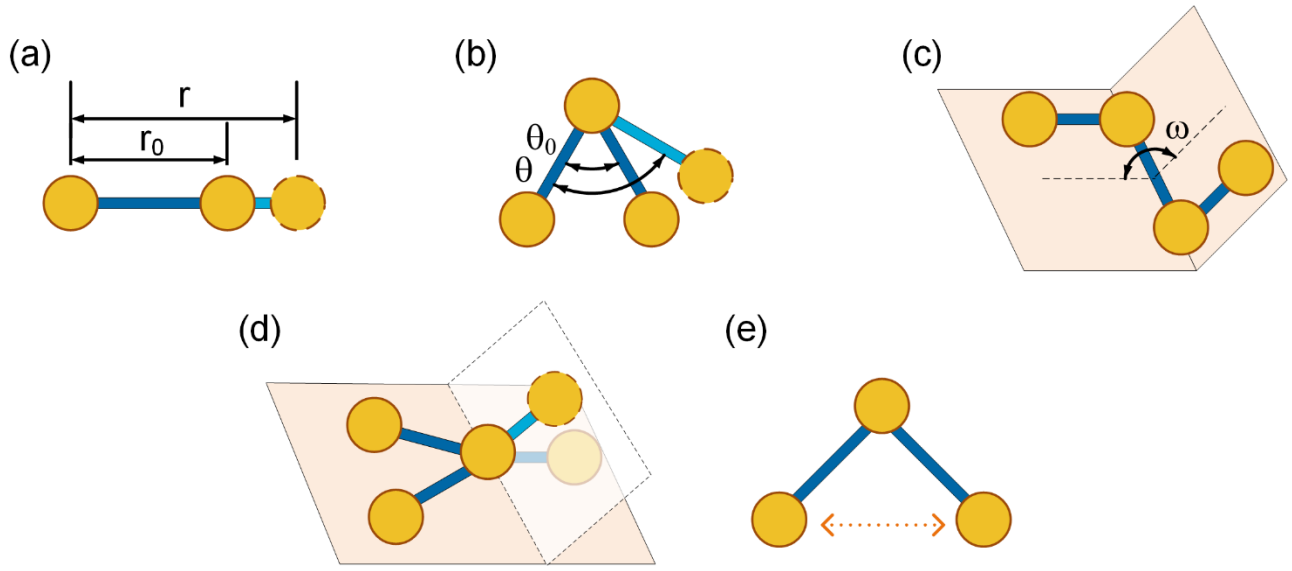

Fig. S6 Illustration of various types of energy involved in molecular mechanics: (a) bond stretching, (b) bond angle, (c) dihedral angle, (d) inversion, and (e) non-bonded

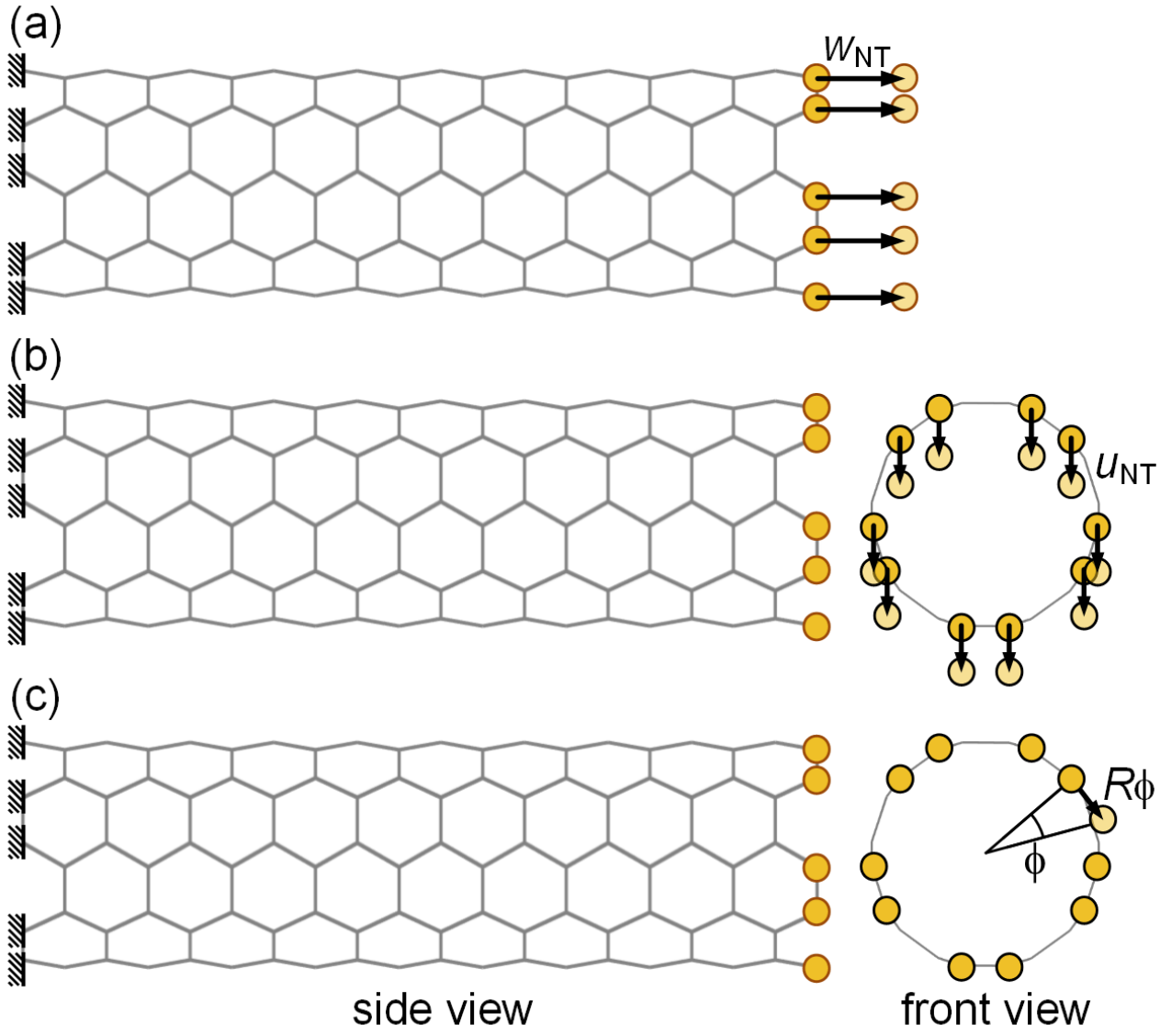

Fig. S7 Illustrations of (a) tensile test with an applied axial displacement, w_{NT}, (b) bending test with an applied transverse displacement, u_{NT}, and (c) torsion test with an applied tangential displacement, $R\varphi$

Supplementary Reference

1. P. Papanikos, D. D. Nikolopoulos and K. I. Tserpes, *Comput. Mater. Sci.*, 2008, **43**, 345-352.